

# Association of Short-Strand DNA Oligomers with Guanidinium-Linked Nucleosides. A Kinetic and Thermodynamic Study

Andrei Blaskó, Robert O. Dempcy, Elvira E. Minyat, and Thomas C. Bruice\*

Contribution from the Department of Chemistry, University of California, Santa Barbara, California 93106

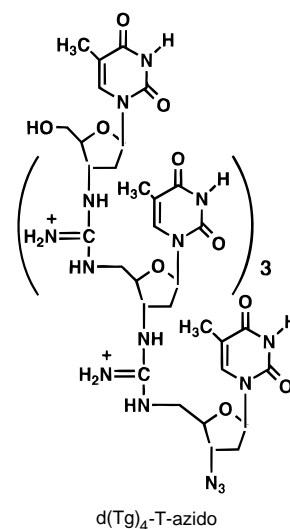
Received April 22, 1996<sup>®</sup>

**Abstract:** Complementary short-strand DNA homooligomers and guanidinium-linked mononucleosides associate and form triplexes in solution. The melting temperatures,  $T_m$ , the association and dissociation kinetic and thermodynamic parameters, and activation energies were determined by UV thermal analysis for the triplexes of short strand DNA homooligomers  $\{d(pA)_5-d(pA)_{12-18}\}$  and poly(dA) with the guanidinium-linked nucleoside  $d(Tg)_4$ -T-azido  $\{DNG_5\}$ . The melting and cooling curves exhibit hysteresis behavior in the temperature range of 5–95 °C at 0.2 deg/min thermal rate. From these curves the rate constants and the energies of activation for association ( $k_{on}$ ,  $E_{on}$ ) and dissociation ( $k_{off}$ ,  $E_{off}$ ) processes were obtained. The  $T_m$  decreases with the ionic strength and increases slightly with increase in concentration of the monomers. A greater increase in the  $T_m$  results from an increase in the length of the DNA strand  $d(pA)_x$ . In the case of  $d(pA)_5$  and  $d(pA)_6$ , triplexes are formed, with  $T_m = 34$  and 39 °C, respectively, only above 0.063 mM/(adenine base) concentration when ionic strength is 0.08. The rate constants  $k_{on}$  and  $k_{off}$  at a reference temperature (288 K) are dependent on the DNA strand length and also decrease and increase respectively with the ionic strength. The energies of activation for the association and dissociation processes are in the range of –10 to –50 and 17 to 44 kcal/mol, respectively. The equilibrium for the formation of the triplexes  $\{(d(Tg)_4\text{-T-azido})_2 \cdot d(pA)_x, x = 5-10\}$  is favored by several orders of magnitude when compared to the triplexes of DNA. The standard molar enthalpies for triplex formation have larger negative values at low ionic strength than at high ionic strength indicating that at lower  $\mu$  values the formation of triplexes of  $d(Tg)_4$ -T-azido with  $d(pA)_x$  is more favored. The values of  $\Delta H^\circ(288)$  calculated from the activation parameters are between –30 and –60 kcal/(mol base) and the values of  $\Delta G^\circ(288)$  are between –8 and –13 kcal/(mol base) for short-strand DNA. There is a linear relationship in the enthalpy–entropy compensation for the triplex-melting thermodynamics.

## Introduction

The negatively charged phosphodiester linkages of double- and triple-stranded DNA and RNA reside side by side causing considerable charge–charge electrostatic repulsion. This is particularly so at the low ionic strength that is physiological. This feature, as well as the susceptibility of DNA and RNA to nuclease activity, limits the usefulness of RNA and DNA as antisense or antigene drugs. P. D. Cook, Y. S. Sanghvi, and co-workers have discussed the desirability of replacing the phosphodiester linkage by other linkages which are either neutral or positively charged, and resistant toward nuclease degradation,<sup>1,2</sup> in order to provide more effective antigene/antisense agents. Also considered by these workers was the desirability in future studies to modify oligonucleotides in such a manner that cellular uptake is enhanced. We have reported the replacement of the phosphate linkages in DNA and RNA by achiral guanido groups which provide a new class of guanidinium (g) linked nucleosides which we identify as DNG and RNG.<sup>3</sup> This paper is focused on the interaction of  $d(Tg)_4$ -T-azido  $\{DNG_5\}$  with complementary short strand DNA oligonucleotides.

The melting temperatures ( $T_m$ ) serve as a measure of the strength of binding of oligonucleotide strands to form duplexes and triplexes. The dynamic processes of thermally induced renaturation and denaturation of double and triple helices are



described by kinetic and thermodynamic parameters. A physicochemical description of biologically important binding interactions of structurally distinct oligonucleotides is thus obtained. For example, the rate of renaturation of DNA's of simpler organisms, such as viruses, is faster than the rate of renaturation of DNA's of more complex organisms, such as bacteria.<sup>4</sup>

In renaturation and denaturation studies reactant single/double strands are in equilibrium with double/triple helical structures at each temperature when the rate of change of temperature is slower than the association and dissociation rates. The association and dissociation rates of triple-helix formation in the case

<sup>®</sup> Abstract published in *Advance ACS Abstracts*, August 15, 1996.

(1) Vasseur, J.-J.; Debart, F.; Sanghvi, Y. S.; Cook, P. D. *J. Am. Chem. Soc.* **1992**, *114*, 4006.

(2) Sanghvi, Y. S.; Cook, P. D. In *Nucleosides and Nucleotides and Antiviral Agents*; Chu, C. K., Baker, D. C., Eds.; Plenum Press: New York, 1993; p 331.

of DNA molecules is slower than in the case of RNA molecules. Thus, at a given rate of heating and cooling and at given temperatures one can see different mole fractions of DNA helical structures dependent on whether one is heating or cooling. Heating and cooling plots of mole fractions *vs* temperature provide a hysteresis.<sup>5</sup> From the shape of the hysteresis curves the individual rates of the association and dissociation of the DNA strands forming duplexes and triplexes and the associated thermodynamic parameters can be determined.

In this study we report the melting temperatures,  $T_m$ , as well as the association and dissociation kinetic and thermodynamic parameters for the formation of triplexes of short strand DNA homooligomers {d(pA)<sub>5</sub>, d(pA)<sub>6</sub>, d(pA)<sub>7</sub>, d(pA)<sub>8</sub>, d(pA)<sub>9</sub>, d(pA)<sub>10</sub>, d(pA)<sub>12–18</sub>} as well as for poly(dA) with d(Tg)<sub>4</sub>-T-azido {DNG<sub>5</sub>}.

## Materials and Methods

The guanidinium-linked oligomer d(Tg)<sub>4</sub>-T-azido was prepared as previously reported.<sup>3a–c</sup> Poly(dA) and d(pA)<sub>5</sub> to d(pA)<sub>10</sub> and d(pA)<sub>12–18</sub> were purchased from Pharmacia Biotech. The concentrations of nucleotide solutions were determined using the extinction coefficients per base {poly(dA)  $\epsilon_{260} = 8400 \text{ M}^{-1} \text{ cm}^{-1}$  and for short d(pA)<sub>x</sub> sequences,  $\epsilon_{257} = 15000 \text{ M}^{-1} \text{ cm}^{-1}$ .<sup>6</sup> For d(Tg)<sub>4</sub>-T-azido we used  $\epsilon_{265} = 8100 \text{ M}^{-1} \text{ cm}^{-1}$ .<sup>3b,c</sup> All experiments were conducted in  $10^{-2} \text{ M}$  phosphate buffer at pH 7.0 and the ionic strength,  $\mu$ , was adjusted with KCl. The concentrations of nucleosides, expressed in M/base, were  $2.1 \times 10^{-5}$  to  $6.3 \times 10^{-5} \text{ M}$  and the ionic strength  $\mu = 0.03–1.20$ . All stock solutions were kept at 4 °C between experiments.

**Sample Preparation.** Six magnetically stirred screw-cap cuvettes of 1 cm path length were used for data collection: five with samples to be measured and one for the temperature monitoring. A layer of Sigmacote (Sigma) was placed above the aqueous reaction solution in order to prevent evaporation and the measurement chamber was purged continuously with dry nitrogen to prevent condensation of water vapor at lower temperatures. Annealing and melting were followed spectrophotometrically.

**UV Spectroscopy and Data Collection.** A Cary 1E UV/vis spectrophotometer equipped with temperature programming and regulation and a thermal melting software package were used for data collection at  $\lambda = 260 \text{ nm}$ . Spectrophotometer stability and  $\lambda$  alignment were checked prior to initiation of each melting point experiment. For the  $T_m$  determinations the hypochromicity was used. Data were recorded every 0.4 deg. The samples were heated from 25 to 95 °C at 5 deg/min, the annealing (95–5 °C) and the melting (5–95 °C) were conducted at 0.2 deg/min, and the samples were brought back to 25 °C at a rate of 5 deg/min. The reaction solutions were equilibrated for 15 min at the highest and lowest temperatures.

**Analysis of Kinetic Data for Triplex Formation.** The equation for triplex formation that was employed<sup>5</sup> (eq 1) describes the formation of the triplex (Tr) from the duplex (D) and the monomer (M), as individual strands. This equation could be interpreted as the reaction



$$K_{\text{eq}} = k_{\text{on}}^T / k_{\text{off}}^T$$

of double-strand D with single-strand M. However, the process of triplex formation may take place in different ways which we shall refer to as domino, normal, and slide (or dangling ends) (Scheme 1). The expression of kinetic equations for the reactants and products (eq 2) can only be accomplished by expressing the concentrations of strands

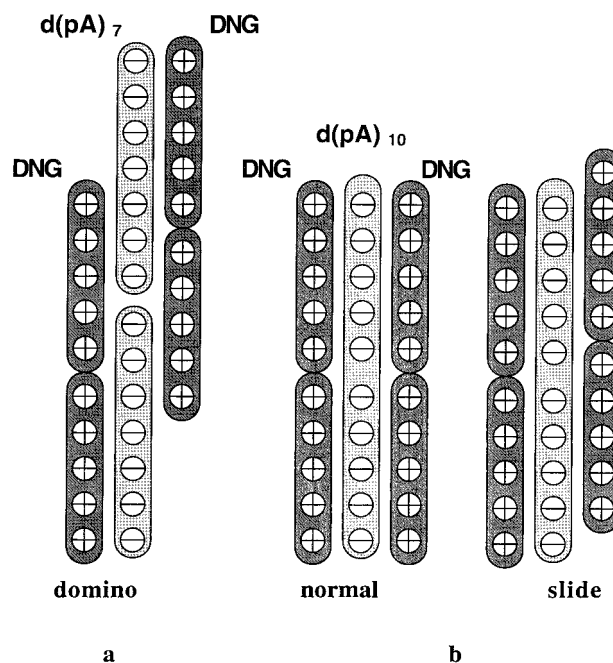
(3) (a) Dempey, R. O.; Almarsson, Ö.; Bruce, T. C. *Proc. Natl. Acad. Sci. U.S.A.* **1994**, *91*, 7864. (b) Dempey, R. O.; Browne, K. A.; Bruce, T. C. *J. Am. Chem. Soc.* **1995**, *117*, 6140. (c) Dempey, R. O.; Browne, K. A.; Bruce, T. C. *Proc. Natl. Acad. Sci. U.S.A.* **1995**, *92*, 6097. (d) Browne, K. A.; Dempey, R. O.; Bruce, T. C. *Proc. Natl. Acad. Sci. U.S.A.* **1995**, *92*, 7051.

(4) Wetmur, J. G.; Davidson, N. *J. Mol. Biol.* **1968**, *31*, 349.

(5) Rougée, M.; Faucon, B.; Mergny, J. L.; Barcelo, F.; Giovannangeli, C.; Garestier, T.; Hélène, C. *Biochemistry* **1992**, *31*, 9269.

(6) Stevens, C. L.; Felsenfeld, G. *Biopolymers* **1964**, *2*, 293.

## Scheme 1



in molar per base (M/base). The theory behind the “on” and “off” rates of the dissociation/association of the triplexes and the derivation of kinetic equations has been described in detail.<sup>5</sup> In eq 1 a triplex is formed from and dissociates to a duplex and a third monomer strand with rate constants  $k_{\text{on}}$  and  $k_{\text{off}}$ . The associated rate for this reaction is given in eq 2. Letting  $D_{\text{tot}} = [D] + [\text{Tr}]$ ; and  $M_{\text{tot}} = [M] + [\text{Tr}]$ ,

$$d[D]/dt = k_{\text{off}}^T [\text{Tr}] - k_{\text{on}}^T [D][M] \quad (2)$$

where the subscript “tot” stands for the total concentration and superscript  $T$  stands for temperature. The monitored absorbance is a weighted combination of the absorbances of the trimer, dimer, and monomer (eq 3) where  $\alpha = [\text{Tr}]/D_{\text{tot}}$ .

$$A = \alpha A_{\text{Tr}} + (1 - \alpha) A_{\text{D+M}} \quad (3)$$

If one defines  $\rho = M_{\text{tot}}/D_{\text{tot}}$ , eq 2 can be written in terms of  $\alpha$  and  $\rho$ :

$$\frac{d\alpha}{dt} = k_{\text{on}}^T M_{\text{tot}} (1 - \alpha) \left(1 - \frac{\alpha}{\rho}\right) - k_{\text{off}}^T \alpha \quad (4)$$

As mentioned in earlier works<sup>5,7,8</sup> the absorbances for the triplex and duplex,  $A_{\text{Tr}}$  and  $A_{\text{D+M}}$  ( $\alpha = 1$  and  $0$ , respectively), are very often temperature dependent. In our determinations, all  $A_{\text{Tr}}$  and  $A_{\text{D+M}}$  baselines were well defined and constant with temperature. Exceptions were in the case of poly(dA). Here we saw a second transition due to the melting of the d(pA)-d(Tg)<sub>4</sub>-T-azido duplex. In this case the short distance between the end of the triplex melting and the beginning of the duplex melting was approximated by a linear  $A_{\text{D+M}}$  temperature dependence. The data points were recorded every 0.4 deg, therefore,  $d\alpha/dt \approx \Delta\alpha/\Delta t = (\alpha_{T+1} - \alpha_{T-1})/0.8$ . In our case we kept the ratio between the duplex and third strand monomer at 1:1 (i.e.,  $\rho = 1$ ) and  $\Delta T/\Delta t = 0.2 \text{ deg/min} = \text{constant}$  for the melting and the cooling processes. To transform eq 4 from a time-dependent into a temperature-dependent equation, both sides should be multiplied by  $dt/dT$  and one can obtain the working equations for the heating (h) and the cooling (c) processes (eqs 5a,b).

$$\frac{d\alpha_h^T}{dT} = \left(\frac{dT}{dt}\right)^{-1} \left\{ k_{\text{on}}^T M_{\text{tot}} (1 - \alpha_h) \left(1 - \frac{\alpha_h}{\rho_h}\right) - k_{\text{off}}^T \alpha_h^T \right\} \quad (5a)$$

(7) Breslauer, K. J.; Sturtevant, J. M.; Tinoco, I., Jr. *J. Mol. Biol.* **1975**, *99*, 549.

(8) Cantor, C. R.; Schimmel, P. R. *Biophysical Chemistry*, Part III; W. H. Freeman and Co.: San Francisco, 1980.

$$\frac{d\alpha_c^T}{dT} = \left(\frac{dT}{dt}\right)^{-1} \left\{ k_{\text{on}}^T M_{\text{tot}} (1 - \alpha_c) \left(1 - \frac{\alpha_c}{\rho_c}\right) - k_{\text{off}}^T \alpha_c^T \right\} \quad (5b)$$

The rate constants  $k_{\text{on}}$  and  $k_{\text{off}}$  are functions of temperature and, therefore, can be expressed as Arrhenius equations:

$$k_{\text{on}} M_{\text{tot}} = k_{\text{on}}^{\text{ref}} M_{\text{tot}} \exp\left[-\frac{E_{\text{on}}}{R} \left(\frac{1}{T} - \frac{1}{T_{\text{ref}}}\right)\right] \quad (6a)$$

$$k_{\text{off}} M_{\text{tot}} = k_{\text{off}}^{\text{ref}} \exp\left[-\frac{E_{\text{off}}}{R} \left(\frac{1}{T} - \frac{1}{T_{\text{ref}}}\right)\right] \quad (6b)$$

where  $R = 1.98 \text{ cal}/(\text{mol}\cdot\text{K})$  and  $T_{\text{ref}}$  any arbitrary temperature. For comparison reasons with other reports<sup>5</sup> we chose  $T_{\text{ref}} = 15 \text{ }^\circ\text{C}$ . In a plot of  $\ln(k_{\text{on/off}})$  vs  $1/T - 1/T_{\text{ref}}$  the thermodynamic parameters  $E_{\text{on/off}}/R$  are obtained as slopes and the kinetic  $k_{\text{on}} M_{\text{tot}}$  and  $k_{\text{off}}$  parameters as intercepts. The variation of the values of  $\alpha$  at the limits restrict the use of this model to the transition portion of the sigmoidal curve. As recognized earlier by others,<sup>5,7,8</sup> the sloping of the baselines and the self-association of the single-stranded oligonucleotides limit the accuracy of the determinations.

**Data Analysis.** The Cary 1E data were exported in ASCII format and smoothed in Matlab (The MathWorks, Inc., Natick, MA) and imported in Mathcad Plus 5.0 (MathSoft, Inc., Cambridge, MA) for calculations and analysis (see supporting information).

## Results

**Melting Curves and Their Hysteresis Behavior.** Melting studies of triplexes formed from short strand DNA homooligomers and  $d(\text{Tg})_4\text{-T-azido}$  have been carried out using UV spectroscopy at 260 nm. The ratio between  $d(\text{Tg})_4\text{-T-azido}$  and  $d(\text{pA})_x$  was 2:1. In Scheme 2 we show the temperature ramping used in these studies. A 15 min waiting period was used at each designated temperature. We have found that all melting curves exhibit hysteresis (Figure 1). The divergence of the heating and cooling curves are functions of the rates of heating and cooling. At 5 deg/min the hysteresis curve is more pronounced, whereas at 0.2 deg/min it is less. Consequently, when  $dT/dt$  approaches zero, the system is at equilibrium, and the melting and the cooling curves coincide such that  $k_{\text{on}} = (\text{constant})k_{\text{off}}$  (eq 4).

**Stoichiometry of the Binding.** Job plots were constructed from absorbances of solutions containing  $d(\text{Tg})_4\text{-T-azido}$  and the DNA homooligomers  $d(\text{pA})_5$  and  $d(\text{pA})_{10}$  in order to assess whether the hysteresis generally seen in the heating and cooling curves (Figure 1) is associated with triplex denaturation. Equilibrated solutions were examined at 10 and 20  $^\circ\text{C}$  (Figure 2). The linear dependence of the absorbances fails below 10% or above 90%  $d(\text{Tg})_4\text{-T-azido}$  but clearly establishes a minima at ca. 67%  $d(\text{Tg})_4\text{-T-azido}$  which corresponds to the formation of a 2:1 ( $d(\text{Tg})_4\text{-T-azido}$ )<sub>2</sub>·(DNA) complex. At 10  $^\circ\text{C}$  the curves are well-defined whereas at 20  $^\circ\text{C}$  the plots are shallow such that it is difficult to define the intersection point of the sloping lines. The same results were obtained at three wavelengths (202, 260, 265 nm). The absorbance change was, however, much larger and the intersection of lines easier to define at 202 nm. It has been reported<sup>6,9-11</sup> that in studies of DNA and RNA oligomers the triplexes are the major absorbing species at 280–284 nm. This report led us to monitor the temperature dependence of absorbance at 284 nm with solutions containing 2:1 and 1:1 ratio of  $d(\text{Tg})_4\text{-T-azido}$  and  $d(\text{pA})_{10}$  (the mole ratio was expressed in per base). The results are displayed in Figure 3 and show a change in absorbance on mixing for only the

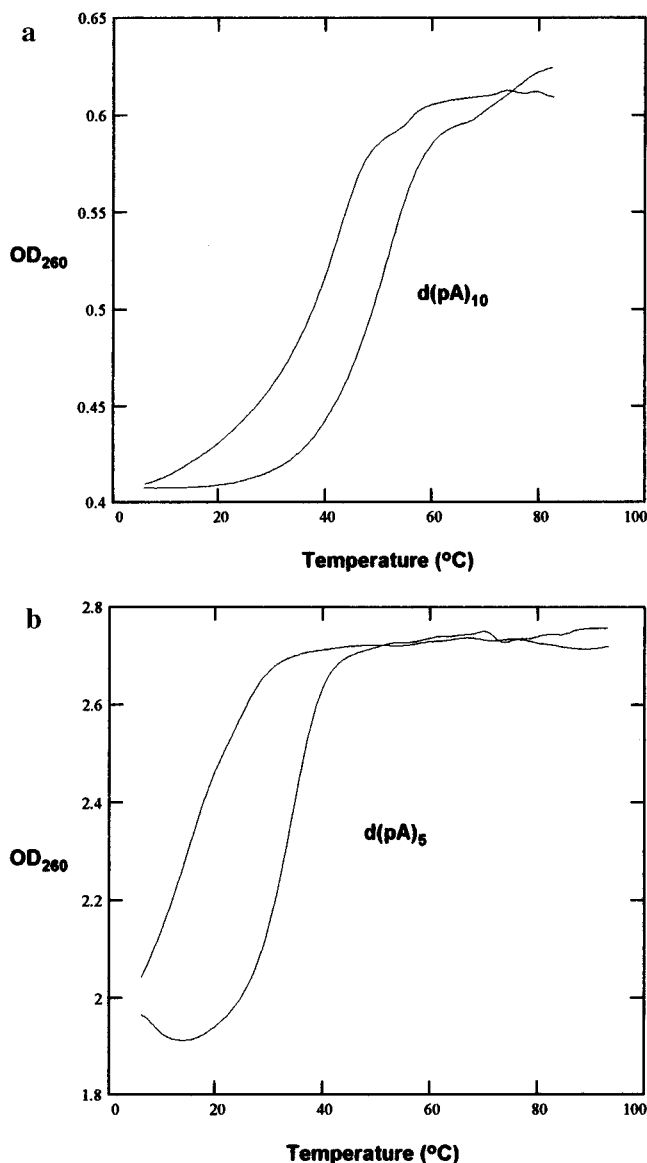
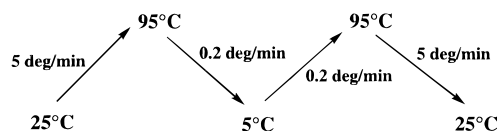


**Figure 1.** Hysteresis curve for the triplex denaturation and renaturation of  $d(\text{pA})_{10}$  (a) and  $d(\text{pA})_5$  (b) with  $d(\text{Tg})_4\text{-T-azido}$  ( $\text{TgXA}\cdot\text{Tg}$ ) at  $2.1 \times 10^{-5}$  and  $6.3 \times 10^{-5}$  M/base of ssDNA respectively at  $\mu = 0.03$ , and 0.2 deg/min heating (cooling) rate. For  $d(\text{pA})_{10}$  a second small transition is observed at  $T_m$  of ca. 76  $^\circ\text{C}$  due to the duplex melting and/or to other types of associations.

## Scheme 2



solution containing the 2:1 stoichiometry, and no changes for the 1:1 stoichiometry when working at  $2.1 \times 10^{-5}$  M/base monomer concentration.

**Effect of the Heating/Cooling Rate.** As the rate of the heating and cooling increases, the rate of equilibration of the species lags such that the hysteresis becomes more marked (Figure 4). These features are shared in the melting characteristics of triplex DNA.<sup>5,12</sup> The four ramps depicted in Scheme 2 can be visualized in Figure 4 as the variation of the absorbance ( $A_{260}$ ) vs temperature. The gap in the hysteresis curve at a heating/cooling rate of 5 deg/min (first and the fourth ramps) is larger than that at a heating/cooling rate of 0.2 deg/min (the

(9) Riley, M.; Maling, B.; Chamberlin, M. J. *J. Mol. Biol.* **1966**, *20*, 359.

(10) Sugimoto, N.; Shintani, Y.; Sasaki, M. *Chem. Lett.* **1991**, 1287.

(11) Sugimoto, N.; Shintani, Y.; Tanaka, A. *Bull. Chem. Soc. Jpn.* **1992**, *65*, 535.

(12) Maher, L. J.; Dervan, P. B.; Wold, B. J. *Biochemistry* **1990**, *29*, 8820.

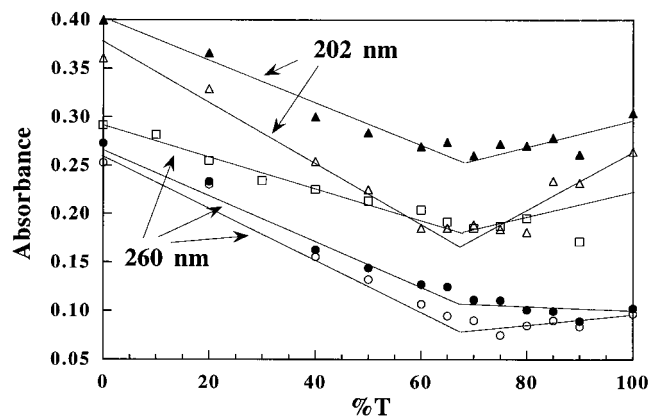


**Figure 2.** Job plots of d(pA)<sub>10</sub> (●, ○, ▲, △) and d(pA)<sub>5</sub> (□) at  $2.1 \times 10^{-5}$  M/base with d(Tg)<sub>4</sub>-T-azido at 10 (open) and 20 °C (solid) at the indicated  $\lambda$  values. As the percentage of T approaches 100, other types of associations could occur.

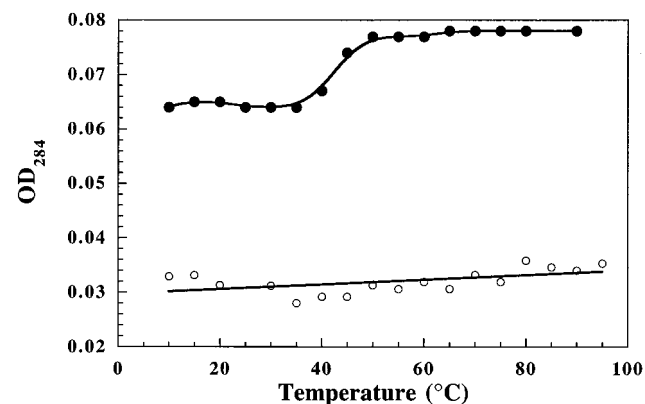


**Figure 3.** Triplex formation at 284 nm between d(Tg)<sub>4</sub>-T-azido and d(pA)<sub>10</sub> (ratio 2:1, solid circles). When the T:A ratio was 1:1 no transition was observed (open circles) due to little or no triplex formation.

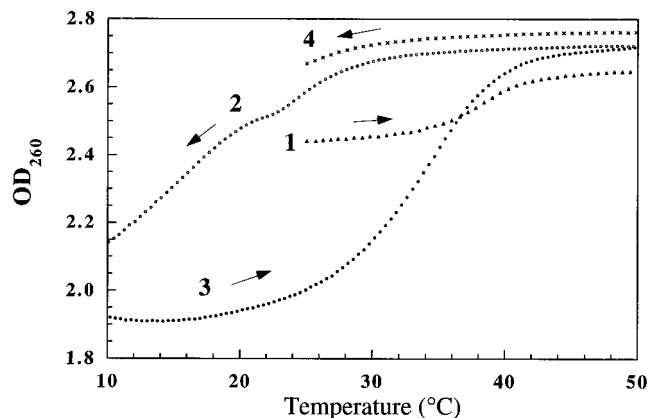


**Figure 4.** Effect of the heating/cooling rate on the extent of association/dissociation of the triplex of d(pA)<sub>5</sub> with d(Tg)<sub>4</sub>-T-azido at  $6.3 \times 10^{-5}$  M/base monomer concentration: (1) fast heating (5 deg/min); (2) slow annealing (0.2 deg/min); (3) slow melting (0.2 deg/min); (4) fast cooling (5 deg/min).

second and the third ramp). At equilibrium, both heating and cooling curves coincide satisfying with the mathematical condition  $d\alpha/dt = 0$  ( $\alpha$  = fraction of duplex engaged in the triplex, see Materials and Methods). Thus from eq 4,  $k_{on}^T M_{tot}(1 - \alpha)(1 - \alpha/\rho) - k_{off}^T \alpha = 0$ . For the cooling curve  $dT/dt < 0$  (we are decreasing the temperature) and  $d\alpha/dt > 0$  (more triplexes are formed in time while cooling; consequently,  $d\alpha/dT < 0$ ). Therefore, the right side of eq 4  $\{k_{on}^T M_{tot}(1 - \alpha)(1 - \alpha/\rho) - k_{off}^T \alpha\}$  is positive and the cooling curve is above the equilibration curve. The opposite is valid for the heating

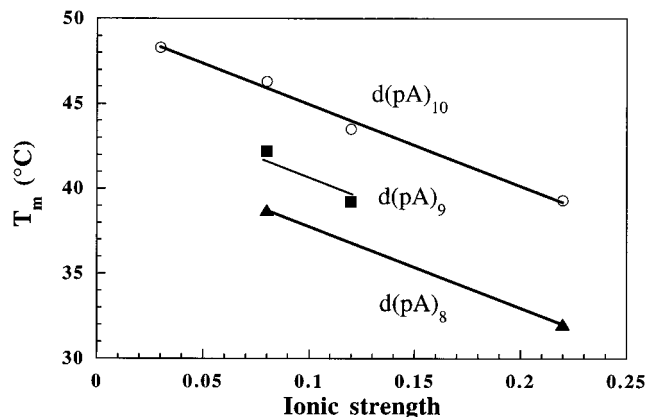


**Figure 5.** Dependence of the  $T_m$  on ionic strength ( $\mu$ ) for the dissociation of triplex formed between d(Tg)<sub>4</sub>-T-azido and d(pA)<sub>x</sub> at  $2.1 \times 10^{-5}$  M/base monomer at the indicated ssDNA lengths. No  $T_m$  determination was possible at this concentrations for d(pA)<sub>5</sub> and d(pA)<sub>6</sub> employed (see text and Table 1). At high ionic strength ( $\mu = 1.2$ ) only poly d(A) forms a triple strand with  $T_m = 37$  °C; for d(pA)<sub>12-18</sub> at  $\mu = 0.06$  the  $T_m$  value was 55 °C (data not shown on the plot).

curve. If the rate of heating/cooling is smaller than the rate of association or dissociation there is no hysteresis and the heating and cooling curves coincide to provide the equilibrium curve.

**Effect of the Ionic Strength on  $T_m$ .** At the concentration of  $2.1 \times 10^{-5}$  M concentration in base A and a 2:1 ratio between the T bases and A bases (in 10 mM phosphate buffer pH 7.0) we saw only one  $T_m$  transition (at 260 nm) after annealing d(Tg)<sub>4</sub>-T-azido with d(pA)<sub>7</sub>, d(pA)<sub>8</sub>, d(pA)<sub>9</sub>, d(pA)<sub>10</sub>, and d(pA)<sub>12-18</sub> (Figure 1). We assigned this transition to the triplex denaturation. In contrast, interaction of d(Tg)<sub>4</sub>-T-azido with poly(dA) exhibits the two transitions corresponding to triplex and duplex melting.<sup>3b,c</sup> We find that only the first transition, corresponding to the triplex denaturation, has hysteresis behavior. With an increase in ionic strength ( $\mu$ ) the value of  $T_m$  decreases (Figure 5). Regardless of the source of dA {i.e., d(pA)<sub>7</sub> to d(pA)<sub>10</sub>}, the slope of a plot of  $T_m$  vs  $\mu$  equals ca.  $-50$  deg/(unit of ionic strength). Above  $\mu = 0.2$  the melting curves become shallow (i.e.,  $\Delta A_{260}$  becomes smaller) and the  $T_m$  determination is less accurate. There is an ionic strength for each DNA length above which transitions cannot be seen or are too shallow to accurately determine the  $T_m$  (see Figure 5). For d(pA)<sub>7</sub> the  $T_m$  determination was possible only at  $\mu = 0.08$ . By increasing the concentration of the dA component to  $6.3 \times 10^{-5}$  M/base and maintaining the 2:1 stoichiometry, we obtained triplexes with d(pA)<sub>5</sub> and d(pA)<sub>6</sub> possessing  $T_m$  values of 34 and 39 °C, respectively [see Figure 1 for d(pA)<sub>5</sub>].

**Kinetics of the Association and Dissociation.** The expression which provides the temperature dependence of the rate constants for association ( $k_{on}$ ) and dissociation ( $k_{off}$ ) is provided in eq 6. At a given reference temperature eq 6 provides  $k_{on}^{ref}$  and  $k_{off}^{ref}$  as well as the activation  $E_{on}$  and  $E_{off}$  parameters. Examination of plots of  $\ln(k_{on} M_{tot})$  and  $\ln(k_{off})$  vs  $1/T$  (Figure 6) shows that in each case there is a linear and a scattered region (see supporting information). The scattered region is associated with the initial and final portions of the triplex melting curve where there is little change in the absorbance, i.e.,  $d\alpha/dt \approx 0$ , which introduces errors. From the intercepts of plots of  $\ln(k_{on} M_{tot})$  and  $\ln(k_{off})$  vs  $1/T - 1/T_{ref}$  we obtain  $k_{on}^{ref} M_{tot}$  and  $k_{off}^{ref}$ , respectively.  $E_{on}/R$  and  $E_{off}/R$  are determined from the respective slopes (Table 1 and Figure 6). Inspection of Table 1 shows that the values of  $k_{on}^{15^\circ C} M_{tot}$  for short-strand DNA oligonucleotides vary between  $6 \times 10^{-4}$  and  $45 \times 10^{-4}$  s<sup>-1</sup> and those of  $k_{off}^{15^\circ C}$  vary between  $0.8 \times 10^{-6}$  and  $37 \times 10^{-6}$  s<sup>-1</sup>. The energies of activation  $E_{on}^{15^\circ C}$  for short-strand oligonucleotides

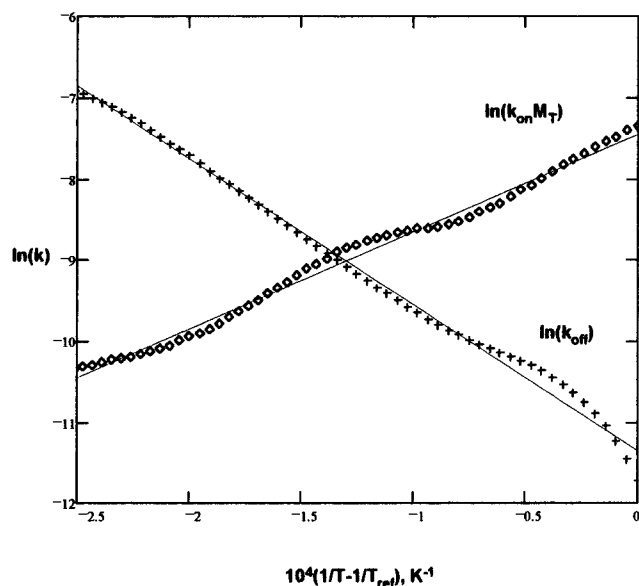


**Figure 6.** Dependence of  $\ln(k_{\text{on}}M_{\text{tot}})$  and  $\ln(k_{\text{off}})$  on  $1/T$  for the denaturation/renaturation of triplex of  $(\text{d}(\text{Tg})_4\text{-T-azido})_2\text{d}(\text{pA})_5$  at  $6.3 \times 10^{-5}$  M/base and  $\mu = 0.08$  and  $dT/dt = 0.2$  deg/min.

**Table 1.** Kinetic and Activation Parameters for the Triplex Melting of  $\text{d}(\text{pA})_x$  with  $\text{d}(\text{Tg})_4\text{-T-azido}^a$

$\mu$	$\text{d}(\text{pA})_x$	$10^5 \text{conc}/$ base (M)	$10^4 k_{\text{on}}^{15^\circ\text{C}} M_{\text{tot}}$ ( $\text{s}^{-1}$ )	$10^6 k_{\text{off}}^{15^\circ\text{C}}$ ( $\text{s}^{-1}$ )	$E_{\text{on}}^{15^\circ\text{C}}$ (kcal/mol)	$E_{\text{off}}^{15^\circ\text{C}}$ (kcal/mol)
1.2	poly d(A)	2.1	19.3	19.4	-34.6	27.5
0.22	$\text{d}(\text{pA})_{10}$	2.1	5.8	35.4	-13.9	17.8
	$\text{d}(\text{pA})_8$	2.1	9.1	37.2	-9.9	16.8
0.12	$\text{d}(\text{pA})_{10}$	2.1	14.3	9.2	-26.7	20.8
	$\text{d}(\text{pA})_9$	2.1	8.4	8.7	-20.8	27.7
0.08	poly d(A)	2.1	$3.2 \times 10^6$	$5.8 \times 10^{-3}$	-49.5	35.2
	$\text{d}(\text{pA})_{12-18}$	2.1	45.2	0.8	-21.8	28.7
	$\text{d}(\text{pA})_{10}$	2.1	16.6	8.6	-29.7	22.2
	$\text{d}(\text{pA})_9$	2.1	5.8	2.0	-24.8	35.6
	$\text{d}(\text{pA})_8$	2.1	5.8	8.7	-22.8	28.7
	$\text{d}(\text{pA})_7$	2.1	8.3	3.7	-34.1	33.3
0.03	$\text{d}(\text{pA})_7$	4.2	20.3	1.6	-15.8	44.4
	$\text{d}(\text{pA})_7$	6.3	28.8	1.4	-19.8	34.7
	$\text{d}(\text{pA})_6$	6.3	14.3	1.8	-25.7	43.6
	$\text{d}(\text{pA})_5$	6.3	5.8	11.8	-23.8	35.6
0.03	$\text{d}(\text{pA})_{10}$	2.1	67.4	2.5	-35.6	27.5

<sup>a</sup> Margin of errors:  $k_{\text{on}}^{15^\circ\text{C}} M_{\text{tot}} = \pm 0.3 \times 10^{-4} \text{ s}^{-1}$ ;  $k_{\text{off}} \pm 0.3 \times 10^{-6} \text{ s}^{-1}$ ;  $E_{\text{on}}^{15^\circ\text{C}}$  and  $E_{\text{off}}^{15^\circ\text{C}} = \pm 0.5 \text{ kcal/mol}$ .

were between -10 and -30 kcal/mol and  $E_{\text{off}}^{15^\circ\text{C}}$  values were between 17 and 44 kcal/mol.

**Influence of the DNA Length on  $k_{\text{on}}$  and  $k_{\text{off}}$ .** The rate constant for the association ( $k_{\text{on}}$ ) of  $\text{d}(\text{Tg})_4\text{-T-azido}$  to  $\text{d}(\text{pA})_x$  increases with increase in  $x$  while the rate constant for the dissociation ( $k_{\text{off}}$ ) decreases (Table 1 and Figure 7). At lower concentration of  $\text{d}(\text{pA})_x$  (e.g.,  $2.1 \times 10^{-5}$  M,  $\mu = 0.08$ ) the rather scattered kinetic data indicate no significant change of  $k_{\text{on}}$  or  $k_{\text{off}}$  with change of chain length up to  $\text{d}(\text{pA})_{10}$ . In the same concentration range,  $k_{\text{on}}$  is one order of magnitude higher and  $k_{\text{off}}$  one order of magnitude lower when the chain length exceeds  $\text{d}(\text{pA})_{10}$  {e.g.,  $\text{d}(\text{pA})_{12-18}$  and poly  $\text{d}(\text{pA})$ }. At the higher concentration of  $\text{d}(\text{pA})_x$  of  $6.3 \times 10^{-5}$  M/base and  $\mu = 0.08$  the dependence of  $k_{\text{on}}$  and  $k_{\text{off}}$  upon chain length is exponential. As the chain length increases {using  $\text{d}(\text{pA})_7$ ,  $\text{d}(\text{pA})_8$ ,  $\text{d}(\text{pA})_9$ ,  $\text{d}(\text{pA})_{10}$ }  $k_{\text{on}}$  increases and  $k_{\text{off}}$  decreases (Table 1).

**Dependence of Kinetic and Activation Parameters on Ionic Strength.** By increasing the ionic strength  $k_{\text{on}}$  increases, while  $k_{\text{off}}$  decreases (Figure 8). The variation of  $k_{\text{on}}$  and  $k_{\text{off}}$  is found to be exponential with change of  $\mu$ . For  $\text{d}(\text{pA})_{10}$  at  $2.1 \times 10^{-5}$  M/base concentration using  $15^\circ\text{C}$  as  $T_{\text{ref}}$ ,  $\Delta k_{\text{on}} M_{\text{tot}} = 55 \times 10^{-4} \text{ s}^{-1}$  and  $\Delta k_{\text{off}} = 32 \times 10^{-6} \text{ s}^{-1}$ . With the ionic

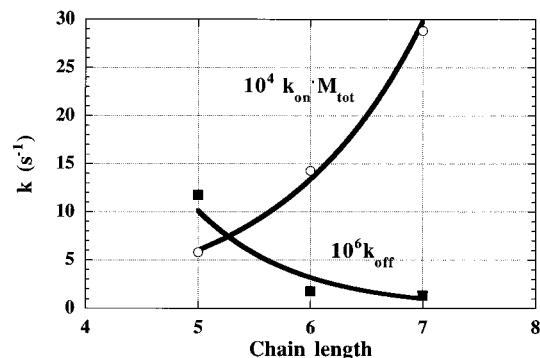


**Figure 7.** Dependence of the  $k_{\text{on}}^{15^\circ\text{C}}$  and  $k_{\text{off}}^{15^\circ\text{C}}$  with the DNA length for the dissociation of the triplex at  $6.3 \times 10^{-5}$  M/base monomer concentration,  $\mu = 0.08$  and  $dT/dt = 0.2$  deg/min.

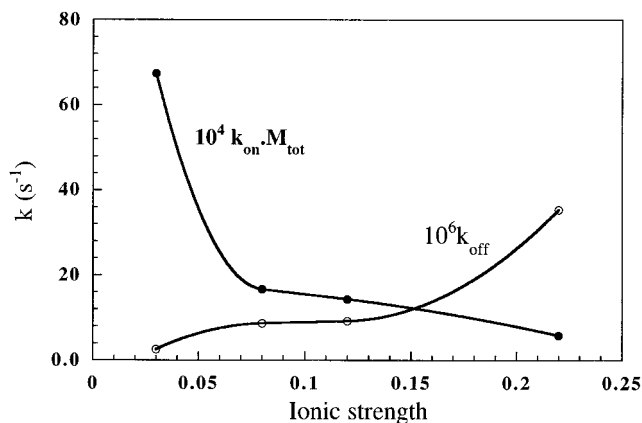


**Figure 8.** Dependence of  $k_{\text{on}}^{15^\circ\text{C}}$  and  $k_{\text{off}}^{15^\circ\text{C}}$  on ionic strength for denaturation/renaturation of the triplex formed from  $\text{d}(\text{pA})_{10}$  ( $2.1 \times 10^{-5}$  M/base) with  $\text{d}(\text{Tg})_4\text{-T-azido}$  ( $4.2 \times 10^{-5}$  M/base) at  $dT/dt = 0.2$  deg/min.

strength decrease (0.22 to 0.08),  $E_{\text{on}}$  decreases from -14 to -30 kcal/mol, whereas  $E_{\text{off}}$  increases from 18 to 28 kcal/mol (Table 1).

**Dependence of Kinetic and Activation Parameters on Concentrations of  $\text{d}(\text{pA})_7$  and  $\text{d}(\text{Tg})_4\text{-T-azido}$ .** At  $\mu = 0.08$ , an increase in  $\text{d}(\text{pA})_7$  concentration from  $2.1 \times 10^{-5}$  M/base to  $6.3 \times 10^{-5}$  M/base, while maintaining the 2:1 ratio between  $\text{d}(\text{Tg})_4\text{-T-azido}$  and DNA, results in an increase in  $k_{\text{on}}^{15^\circ\text{C}} M_{\text{tot}}$  from  $8.3 \times 10^{-4}$  to  $28.8 \times 10^{-4} \text{ s}^{-1}$ , i.e.,  $k_{\text{on}}^{15^\circ\text{C}} \approx 42 \text{ M}^{-1} \text{ s}^{-1}$  (molarity in per base), whereas  $k_{\text{off}}^{15^\circ\text{C}}$  does not change significantly (Table 1). No significant dependence of  $E_{\text{on}}$  and  $E_{\text{off}}$  on the DNA length was found in the DNA concentrations and the ionic strength range studied.

## Discussion

Replacement of the phosphodiester linkages of the DNA with guanidine linkages provides the polycation deoxyribonucleic guanidine (DNG). The  $\text{d}(\text{Tg})_4\text{-T-azido}$  polycation binds to poly(dA) and poly(rA) with unprecedented affinity and with base-pair specificity to provide both double- and triple-stranded helices.<sup>3b-d</sup> Positively charged  $\text{d}(\text{Tg})_4\text{-T-azido}$  has a significantly greater affinity for poly(dA) and poly(rA) than the DNA equivalent. The effect of ionic strength on melting is more pronounced with  $\text{d}(\text{Tg})_4\text{-T-azido}$  interacting with  $\text{d}(\text{pA})_x$  and has an opposite effect as compared to DNA complexes with DNA or RNA. This is due, of course, to electrostatic interactions being attenuated by increasing salt concentrations.<sup>3b</sup> Earlier works in this laboratory show that the  $T_m$  of the double helix of pentameric thymidyl DNA with poly(dA) at  $\mu = 0.12$  is ca.  $13^\circ\text{C}$ , whereas the  $\text{d}(\text{Tg})_4\text{-T-azido}$  duplex with poly(dA) does not dissociate in boiling water.<sup>3c</sup> At an ionic strength of 0.22

the five bases of d(Tg)<sub>4</sub>-T-azido were estimated to dissociate from a double helix with poly(rA) at >100 °C.<sup>3d</sup> The recognition of adenine by d(Tg)<sub>4</sub>-T-azido, as opposed to guanine and cytosine, makes this class of positively charged nucleosides putative antisense/antigenic agents.

The melting studies of complexes formed from short-strand DNA homooligomers and d(Tg)<sub>4</sub>-T-azido showed that all melting curves exhibit hysteresis (Figure 1) at the rate of heating-cooling employed (0.2 deg/min). Rates of heating and cooling of up to 0.5 deg/min are generally slow enough to ensure attainment of the equilibrium in the case of duplex to coil transitions in oligonucleotides, i.e., heating and cooling curves coincide.<sup>5</sup> Association and dissociation kinetics for the oligodeoxyribonucleotide 5'-CTCTTTCCTCTCTTTTCCCC (bold C's indicate 5-methylcytosine residues) binding to pMTCAT-TH1, supercoiled plasmid DNA, at 1 nM concentration, show that the value of the observed pseudo-first-order association rate constant,  $k_{2\text{obs}}$ , is  $1.8 \times 10^3 \text{ M}^{-1} \text{ s}^{-1}$ .<sup>12</sup> The half-life for the triplex formation for pRW2322 and pRW2325 supercoiled plasmids at 37 °C was found to be 0.5–4 min corresponding to a  $k_{\text{obs}}$  of 0.003–0.02 s<sup>-1</sup>.<sup>13</sup> Hysteresis behavior at a heating-cooling rate of 0.1–0.5 deg/min was found for the melting of triplexes of short-strand (22 base pairs) DNA oligomers as well.<sup>5</sup> At a heating-cooling rate of 0.2 deg/min, we observed hysteresis between heating and cooling curves, the magnitude being a function of the rates of heating and cooling. This points to the existence of triplexes between d(Tg)<sub>4</sub>-T-azido and d(pA)<sub>x</sub>. Previous melting studies with poly(dA) and d(Tg)<sub>4</sub>-T-azido established the existence of two transitions corresponding to melting of triplex and duplex.<sup>3b,c</sup> Our present results show that only the first transition, corresponding to the triplex denaturation, exhibits hysteresis behavior. Supporting evidence for triplex formation comes from the use of the continuous variation method. The minima observed in Figure 2 occurs at ca. 67% d(Tg)<sub>4</sub>-T-azido demonstrating the existence of the (d(Tg)<sub>4</sub>-T-azido)<sub>2</sub>·(DNA) complex. The observation that at 10 °C the curves are well defined whereas at 20 °C the plots are shallow shows that the process of triplex formation is highly dynamic and is favored at lower temperatures. With dsDNA the maximum rate of renaturation usually occurs at a temperature of 20 to 30 °C below the melting temperature ( $T_m$ ).<sup>4</sup> The reversibility of the formation of triplexes was studied by Felsenfeld and co-workers,<sup>14</sup> who recognized that the sharpness of the mixing curves was related to the extent of complex formation (to concentration of reactants and temperature). To further support the formation of (d(Tg)<sub>4</sub>-T-azido)<sub>2</sub>·(DNA) triplex we used a discriminating wavelength (284 nm) at which the triplexes are the major absorbing species.<sup>6,9</sup> The hypochromicity of the melting curves at 284 nm for the 2:1 stoichiometry and the isochromicity of the melting curves for the 1:1 stoichiometry ( $2.1 \times 10^{-5} \text{ M}$ /base monomer concentration) are consistent with the existence of the (d(Tg)<sub>4</sub>-T-azido)<sub>2</sub>·(DNA) complex (Figure 3). However, due to the small OD change and the measurements' accuracy, this wavelength should be used cautiously and not used to define kinetic and thermodynamic parameters.

Since electrostatic interactions play a key role in the formation of the complexes of d(Tg)<sub>4</sub>-T-azido hybrids with DNA or RNA, these interactions are attenuated by increasing salt concentrations.<sup>3b</sup> This phenomenon reverses the ionic strength effect on the  $T_m$  values of d(Tg)<sub>4</sub>-T-azido hybrids with DNA or RNA as compared to DNA complexes with DNA or RNA (Figure 5). The reaction of DNG with DNA or RNA is favored at physiologic ionic strength whereas the complexing of DNA by DNA or RNA is not. By inspection of Figure 5, the plot of  $T_m$

**Table 2.** Thermodynamic Parameters for the Triplexes of d(pA)<sub>x</sub> with d(Tg)<sub>4</sub>-T-azido

$\mu$	d(pA) <sub>x</sub>	10 <sup>5</sup> conc/ base (M)	$\Delta H^\circ(288)^{a,b}$ (kcal/mol)	$\Delta S^\circ$ <sup>c</sup> (cal/ (mol·K))	$\Delta G^\circ(288)^d$ (kcal/mol)	$T_m^e$ (°C)
0.22	d(pA) <sub>10</sub>	2.1	-31.7	-79	-9.0	39.3
	d(pA) <sub>8</sub>	2.1	-26.7	-65	-8.0	32 <sup>e</sup>
0.12	d(pA) <sub>10</sub>	2.1	-47.5	-127	-10.8	43.5
	d(pA) <sub>9</sub>	2.1	-48.5	-133	-10.3	39.2
0.08	d(pA) <sub>10</sub>	2.1	-51.9	-140	-11.6	46.3
	d(pA) <sub>9</sub>	2.1	-60.4	-169	-11.8	42.2
	d(pA) <sub>8</sub>	2.1	-51.5	-142	-10.5	38.7
	d(pA) <sub>7</sub>	2.1	-59.4	-168	-10.9	37.1
	d(pA) <sub>7</sub>	4.2	-60.2	-169	-11.5	40.7
	d(pA) <sub>7</sub>	6.3	-56.4	-154	-12.0	45.8
0.03	d(pA) <sub>6</sub>	6.3	-69.3	-199	-11.9	39 <sup>e</sup>
	d(pA) <sub>5</sub>	6.3	-59.4	-171	-10.2	34 <sup>e</sup>
	d(pA) <sub>10</sub>	2.1	-63.2	-174	-13.1	48.3

<sup>a</sup> From  $E_{\text{on}} - E_{\text{off}}$ .<sup>5</sup> <sup>b</sup>  $\pm 0.2$  kcal/mol. <sup>c</sup>  $\pm 1$  cal/(mol·K). <sup>d</sup>  $\pm 0.3$  °C. <sup>e</sup>  $\pm 1$  °C.

vs  $\mu$  has a slope of ca. -50 deg/(unit of ionic strength). This relatively large value is a measure of the pronounced ionic strength effect on  $T_m$ . The observation of triplexes on reaction of d(Tg)<sub>4</sub>-T-azido with d(pA)<sub>5</sub> and d(pA)<sub>6</sub> at  $6.3 \times 10^{-5} \text{ M}$ /base which possess  $T_m$  values of 34 and 39 °C, respectively (Figure 1 and Table 2), is most remarkable. Triplexes of such short oligos have not been observed with d(pT)<sub>5</sub> + d(pA)<sub>5</sub> showing the unprecedented affinity of d(Tg)<sub>4</sub>-T-azido toward d(pA)<sub>x</sub>.

The triplex forms and dissociates to a duplex and a third monomer strand with rate constants  $k_{\text{on}}$  and  $k_{\text{off}}$  (eq 1). The kinetic equations could be very complicated if we consider that unoccupied sites could exist {e.g., d(pA)<sub>7</sub> + 2 DNG<sub>5</sub>, Scheme 1}. Even in the case of d(pA)<sub>10</sub> where we expect to have fully occupied (-) sites by two molecules of d(Tg)<sub>4</sub>-T-azido there can be slides of the strands (Scheme 1b), but here and elsewhere<sup>5,7</sup> species other than full associations are neglected (all-or-none model) in the kinetic and thermodynamic studies. Some small corrections pertain to the fraying of the end bases of the complexes.<sup>15</sup> The fact that there is little or no sloping of the baseline demonstrates that the self association of the single strands is negligible.<sup>16</sup>

At 15 °C the second-order rate constant,  $k_{\text{on}}$ , for the triplex formation with short-strand (5–10) oligonucleotides is 30–200 M<sup>-1</sup> s<sup>-1</sup> (the molarity is expressed in per bases) and the first-order rate constant  $k_{\text{off}}$  is  $0.1\text{--}3 \times 10^{-5} \text{ s}^{-1}$  in the range of  $\mu = 0.03\text{--}0.22$ . It is most interesting to note that the  $k_{\text{on}}$  values for DNG<sub>5</sub> are, on average, one order of magnitude larger than those found for a DNA triplex having the length of 22 bp at [NaCl] = 0.02–0.30 M.<sup>5</sup> On the other hand, the  $k_{\text{off}}$  values are of the same order of magnitude as seen with a DNA triplex having the length of 22 bp. This comparison is only qualitative since the ionic strength acts in opposite direction and the composition of the 22 DNA oligonucleotide alluded to differs from the short-strand DNA oligonucleotides in this study. For a given DNA strand at a fixed concentration and ionic strength, a decrease in the molecular weight results in a decrease in the rate of renaturation.<sup>4</sup> The second-order rate constant,  $k_{\text{on}}$ , increases one order of magnitude and the first-order rate constant,  $k_{\text{off}}$ , decreases one order of magnitude when the chain length exceeds d(pA)<sub>10</sub> (*vide supra*). We can conclude that the association of d(Tg)<sub>4</sub>-T-azido with d(pA)<sub>5</sub> up to d(pA)<sub>10</sub> is very strong and one can estimate that it far exceeds that of its DNA counterpart by at least three orders of magnitude.

As in the case of DNA duplexes and triplexes, the association of the strands decreases as the oligomer strand becomes shorter.

(13) Kang, S.; Wohrlab, F.; Wells, R. D. *J. Biol. Chem.* **1992**, *267*, 19435.

(14) Felsenfeld, G. *Biochim. Biophys. Acta* **1958**, *29*, 133.

(15) Gralla, J.; Crothers, D. M. *J. Mol. Biol.* **1973**, *78*, 301.

(16) Vesnaver, G.; Breslauer, K. J. *Proc. Natl. Acad. Sci. U. S. A.* **1991**, *88*, 3569.

The second-order rate constant for reaction of  $d(\text{Tg})_4$ -T-azido with  $d(\text{pA})_x$ ,  $k_{\text{on}}$ , increases with increase in  $x$  while the first-order rate constant,  $k_{\text{off}}$ , decreases (Figure 7 and Table 1). This dependence is better visualized at the higher concentration of  $d(\text{pA})_x$ , e.g.,  $6.3 \times 10^{-5}$  M/base and  $\mu = 0.08$ .

There is a close relationship between the  $T_m$  values and the kinetic and activation parameters for the triplex formation because ultimately they describe the strength of association. As expected, by decreasing the ionic strength  $k_{\text{on}}$  increases, while  $k_{\text{off}}$  decreases (Figure 8). As one changes  $\mu$  the variation of  $k_{\text{on}}$  and  $k_{\text{off}}$  is found to be exponential. The fact that the sensitivity of  $k_{\text{on}}$  to  $\mu$  is about twice that of  $k_{\text{off}}$  is not surprising since in the case of DNA triplexes  $k_{\text{off}}$  has no ionic strength dependence.<sup>5</sup> The existence of the ionic strength dependence on  $k_{\text{off}}$  is ascribed to the fact that the electrostatic phenomena are more pronounced in the case of the association of  $d(\text{Tg})_4$ -T-azido with DNA than in the case of DNA triplexes. The same trend has been found for the activation parameters,  $E_{\text{on}}$  and  $E_{\text{off}}$ . For  $d(\text{pA})_{10}$ , with decrease in ionic strength  $E_{\text{on}}$  decreases from  $-14$  to  $-30$  kcal/mol, whereas  $E_{\text{off}}$  increases from  $18$  to  $28$  kcal/mol (Table 1). A more negative  $E_{\text{on}}$  at low ionic strength and a more positive value of  $E_{\text{off}}$  favors a better association at low  $\mu$  values.

There is a concentration dependence of the kinetic parameters for triplex formation. The second-order rate constant  $k_{\text{on}}^{15^\circ\text{C}} \approx 42 \text{ M}^{-1} \text{ s}^{-1}$  (molarity in per base) remains constant on increase in  $d(\text{pA})_7$  concentration by a factor of 3, while maintaining the 2:1 ratio between  $d(\text{Tg})_4$ -T-azido and DNA. There was no significant change in  $k_{\text{off}}^{15^\circ\text{C}}$  (Table 1). This is an indication that there are no intramolecular associations, because an intramolecular reaction is concentration independent.

An interesting feature of the triplex formation between  $d(\text{Tg})_4$ -T-azido and  $d(\text{pA})_x$  is the observation of only one transition between  $5$  and  $95^\circ\text{C}$ ! The addition of up to 30% ethanol is known to decrease  $T_m$  values.<sup>17</sup> Our attempt to observe a second transition by ethanol addition was not successful (data not shown). We observed a decrease of  $10$ – $20^\circ\text{C}$  in  $T_m$  values for the triplex with no significant change of the upper plateau of the melting curves. This can be interpreted as follows: (a) the second transition exceeds the boiling point of the water; (b) the duplex transition is too small as compared to the triplex transition and is contained in the main triplex melting curve; and (c) the triplex melts to three single strands *via* a less stable duplex. There are dodecamer hybrid triplexes of RNA and DNA which melt from triplex to single strand. For example, the homopolymer pair  $\text{rA}\cdot\text{rU}$  is not stable under any conditions of temperature and salt concentration tested. Mixtures of  $\text{dA}$  with  $\text{rU}$  contain three-stranded  $\text{dA}\cdot\text{rU}_2$  as the only helical complex.<sup>9</sup> In general relatively unstable DNA duplexes form particularly stable triplexes and *vice versa*.<sup>18</sup>

The interest in thermodynamic data on nucleic acids intensified when it was shown that the thermal stabilities depend not only on base composition but also on nucleotide sequence.<sup>19</sup> The variation in stability of short DNA or RNA double and triple helices falls over a range of  $>10$  kcal/mol.<sup>18</sup> In forming the triple helix, RNA is favored on both pyrimidine strands, whereas DNA is favored on the purine strand.

Double- and triple-helix stabilities can be described in terms of the standard free energy,  $\Delta G^\circ = \Delta H^\circ - T\Delta S^\circ$ ,<sup>20</sup> if one knows the standard enthalpy and entropy changes ( $\Delta H^\circ$  and  $\Delta S^\circ$ ) for the melting of each nearest-neighbor doublet of base pairs in

DNA.<sup>21</sup> The thermodynamic parameters can be extracted from the kinetic data or can be experimentally determined by calorimetric methods. In many cases these data obtained by different methods are in good agreement.<sup>22</sup> However, single-stranded DNA, as well as RNA bases, are stacked resembling a single strand of a double helix and they bring their own energy contributions in forming duplexes and triplexes<sup>23</sup> and the actual enthalpies of duplex and triplex formation could be lower due to the fact that the strands are already in a helical conformation.<sup>16</sup> In many cases stacking interactions are more important than pairing interactions in determining the stability of the terminal base pairs,<sup>24</sup> which in the case of short-strand oligonucleotides play a key role. Although the thermodynamic contribution of DNA single-stranded orders to the thermally induced disruption of their corresponding duplex is small, their enthalpies of formation could contain up to 40% of the ssDNA enthalpies that ultimately stabilizes the final duplex state.<sup>16</sup> This fact brings up the enthalpy–entropy compensation in the formation of the DNA complexes. The enthalpy–entropy compensation at the conventional temperature,  $T = 298.15$  K, for the duplex melting<sup>21</sup> can be formulated in terms of eq 7 and is related to  $T_m$  by eq 8, where  $T_o = 275$  K, and  $a = 81$  cal/(mol·K).

$$\Delta S^\circ = a\Delta H^\circ/(aT_o + \Delta H^\circ) \quad (7)$$

$$T_m = T_o + \Delta H^\circ/a \quad (8)$$

Experimental enthalpies for formation of DNA triplexes from duplexes and single strands range from ca.  $-2$  to  $-7$  kcal/(mol of base).<sup>25</sup> The  $\Delta H_i$  (ionization) of the buffer and the pH used in the experiments influence the observed triplex thermodynamic parameters. Unlike the results with the mixed sequences, the  $T_m$  values and calorimetric  $\Delta H$  for triplex formation from the A·T duplex are independent of pH and buffer species. Equations 7 and 8 could be applied to the triplexes as well, however, the parameters  $a$  and  $T_o$  should be determined for the new system. Equation 9 shows the relationship between the thermodynamic parameters  $\Delta H^\circ$  and  $\Delta S^\circ$  and the equilibrium constant,  $K_{\text{eq}}$ , at a given temperature.

$$\Delta H^\circ - T\Delta S^\circ = -RT \ln K_{\text{eq}}(T) \quad (9)$$

At the melting temperature,  $T_m$ ,  $K_{\text{eq}} = 2/M_{\text{tot}}^5$  and at  $288$  K  $K_{\text{eq}}$  is given by  $k_{\text{on}}^{\text{ref}}/k_{\text{off}}^{\text{ref}}$ . From eq 9 one can calculate the standard molar entropies for the triplex formation and from eq 10 the free energies of formation,  $\Delta G^\circ$  (Table 2).

$$\Delta G^\circ = \Delta H^\circ - T\Delta S^\circ \quad (10)$$

The standard molar enthalpies have larger negative values at low ionic strength than at high ionic strength in accord with the observation that at lower  $\mu$  values the formation of triplexes of  $d(\text{Tg})_4$ -T-azido with  $d(\text{pA})_x$  is more favored. The standard molar enthalpies  $\Delta H^\circ(288) = E_{\text{on}} - E_{\text{off}}$  are between  $-30$  and  $-60$  kcal/(mol base) for short strands ( $5$ – $10$  base pairs, Table 2) as compared to  $-120$  kcal/(mol strand) for a 22 base-pair DNA triplex.<sup>5</sup> Sugimoto and co-workers have determined the thermodynamic parameters for the RNA/DNA hybrid duplexes and showed that pentameric hybrid duplexes with different

(21) Petruska, J.; Goodman, M. F. *J. Biol. Chem.* **1995**, *270*, 746.

(22) Albergo, D. P.; Marky, L. A.; Breslauer, K. K.; Turner, D. H. *Biochemistry* **1981**, *20*, 1409.

(23) Cantor, C. R.; Warsaw, M. M.; Shapiro, H. *Biopolymers* **1970**, *9*, 1059.

(24) Petersheim, M.; Turner, D. H. *Biochemistry* **1983**, *22*, 256.

(25) Wilson W. D.; Hopkins, H. P.; Mizan, S.; Hamilton, D. D.; Zon, G. *J. Am. Chem. Soc.* **1994**, *116*, 3607.

(17) Ivanov, V. I.; Krylov, D. Yu.; Minyat, E. E. *J. Biomol. Struct. Dynam.* **1985**, *3*, 43.

(18) Roberts, R. W.; Crothers, D. M. *Science* **1992**, *258*, 1463.

(19) Breslauer, K. J. In *Thermodynamic Data for Biochemistry and Biotechnology*; Hinz, H.-J., Ed., Springer-Verlag: Berlin, 1986; Chapter 15.

(20) Marky, L. A.; Breslauer, K. J. *Biopolymers* **1987**, *26*, 1601.

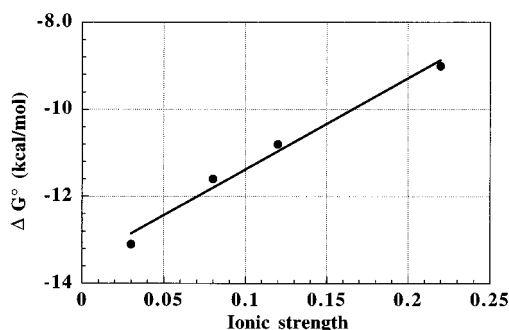


**Figure 9.** Dependence of  $\Delta G^\circ$  on ionic strength for the  $(d(\text{Tg})_4\text{-T-azido})_2 \cdot d(\text{pA})_{10}$  complex formation.

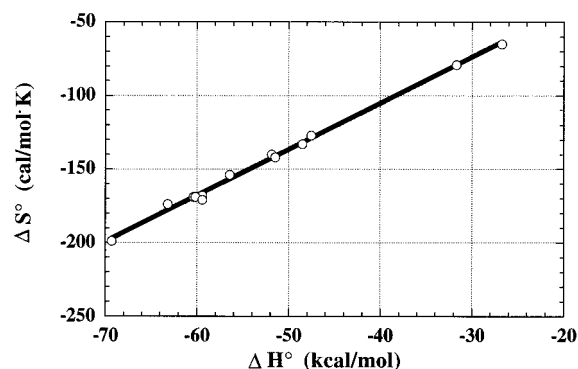


**Figure 10.** Enthalpy–entropy compensation in the triplex  $\{(d(\text{Tg})_4\text{-T-azido})_2 \cdot (\text{DNA})\}$  melting thermodynamics.

mixed base sequences have  $\Delta H^\circ$  of ca.  $-45$  kcal/(mol strand).<sup>26</sup> These large and negative values of  $\Delta H^\circ(288)$  indicate a better stabilization of the  $(d(\text{Tg})_4\text{-T-azido})_2 \cdot (\text{DNA})$  complex as compared with the DNA triplexes with at least one order of magnitude on the enthalpy scale even with the entropy compensation. Triplex formation between  $d(\text{Tg})_4\text{-T-azido}$  and  $d(\text{pA})_x$  is associated with values of  $\Delta G^\circ$  ranging between  $-8$  and  $-13$  kcal/mol with large negative values at low ionic strengths (Table 2 and Figure 9). The  $\Delta G^\circ$  values of formation of the  $(d(\text{Tg})_4\text{-T-azido})_2 \cdot (\text{DNA})$  are ca. two times lower compared to  $\Delta G^\circ$  values for the RNA/DNA hybrid pentameric duplexes<sup>26</sup> denoting a better stabilization of the latter. A plot of  $\Delta S^\circ$  vs  $\Delta H^\circ$  shows a linear dependence (Figure 10) and can be related to the enthalpy–entropy compensation earlier reported in the DNA duplexes melting thermodynamics which follow a rectangular hyperbola.<sup>21</sup> It is clear that more sequence-dependent kinetic and thermodynamic data on the stability and conformational flexibility of all secondary structural features (e.g., internal loops, bulges, etc.) are required<sup>19</sup> to assess the potential role of these structures in biological events such as frameshift mutagenesis, drug binding, and protein–nucleic acid interactions.

## Conclusions

Replacement of the phosphodiester linkages of DNA with guanidine linkages provides a polycation deoxyribonucleic guanidine (DNG). The polycation  $d(\text{Tg})_4\text{-T-azido}$  binds to poly(dA) and poly(rA) with unprecedented affinity and with base-pair specificity to provide both double- and triple-stranded helices. The melting studies of complexes formed from short-strand DNA homooligomers and  $d(\text{Tg})_4\text{-T-azido}$  showed, in all cases, that plots of melting and annealing curves exhibit hysteresis the magnitude of which is dependent upon the heating and cooling rates. Further, there can be observed only one transition between 5 and 95 °C. This transition relates to the

formation and melting of triple-helix structures composed of  $d(\text{Tg})_4\text{-T-azido}$  and  $d(\text{pA})_x$ . Job plots (continuous variation method) establish the stoichiometry as  $(d(\text{Tg})_4\text{-T-azido})_2 \cdot d(\text{pA})_x$ . In general the Job plots are well defined at 10 °C whereas at 20 °C the plots are shallow. Also the hypochromicity of the melting curves at 284 nm for the 2:1 stoichiometry and the isochromicity of the melting curves for the 1:1 stoichiometry ( $2.1 \times 10^{-5}$  M/base monomer concentration) are consistent with the existence of the  $(d(\text{Tg})_4\text{-T-azido})_2 \cdot d(\text{pA})_x$  complex. The electrostatic attraction between polycation  $d(\text{Tg})_4\text{-T-azido}$  and polyanion  $d(\text{pA})_x$  stabilizes the helical hybrid structures. Increase in ionic strength decreases this electrostatic interaction and lowers the value of  $T_m$ . In the interaction of  $d(\text{Tg})_4\text{-T-azido}$  with  $d(\text{pA})_x$ , increase in ionic strength provides a negative slope of a plot of  $T_m$  vs  $\mu$  of ca.  $-50$  deg/(unit of ionic strength). The magnitude of the ionic strength effect on  $T_m$  in the case of  $(d(\text{Tg})_4\text{-T-azido})_2 \cdot d(\text{pA})_x$  triplex is much greater than observed with complexes with short strand DNA oligos. At a concentration of  $6.3 \times 10^{-5}$  M/(base A) and at a stoichiometry of 2:1 T/A one observes triplexes with  $d(\text{pA})_5$  and  $d(\text{pA})_6$  possessing  $T_m$  values of 34 and 39 °C, respectively. Such thermodynamically favored association has not been seen in the interaction of  $d(\text{pT})_5$  such that  $d(\text{Tg})_4\text{-T-azido}$  shows an unprecedented affinity toward  $d(\text{pA})_x$ .

The triplex forms and dissociates to a duplex and a third monomer strand with rate constants  $k_{\text{on}}$  and  $k_{\text{off}}$ . At 15 °C and in the range of ionic strengths of 0.03–0.22, the second-order rate constant ( $k_{\text{on}}$ ) for the triplex formation with short-strand oligonucleotides  $\{d(\text{pA})_x$ , where  $x = 5, 6, 7, 8, 9$ , and  $10\}$  is  $30\text{--}200$   $\text{M}^{-1} \text{s}^{-1}$  (the molarity is expressed in per bases) and the first-order rate constant ( $k_{\text{off}}$ ) is  $0.1\text{--}3 \times 10^{-5}$   $\text{s}^{-1}$ . The value of  $k_{\text{on}}$  for reaction of  $d(\text{Tg})_4\text{-T-azido}$  with  $d(\text{pA})_x$  increases with increase in  $x$  while the rate constant  $k_{\text{off}}$  decreases. This dependence is better visualized at the higher concentration of  $d(\text{pA})_x$ , e.g.,  $6.3 \times 10^{-5}$  M/base and  $\mu = 0.08$ . By decreasing the ionic strength  $k_{\text{on}}$  increases, while  $k_{\text{off}}$  decreases. The same trend has been found for the activation parameters,  $E_{\text{on}}$  and  $E_{\text{off}}$ . For  $d(\text{pA})_{10}$ , with decrease in ionic strength there is a decrease in  $E_{\text{on}}$  from  $-14$  to  $-30$  kcal/mol, whereas  $E_{\text{off}}$  increases from 18 to 28 kcal/mol. A more negative  $E_{\text{on}}$  at low ionic strength and a more positive value of  $E_{\text{off}}$  favors association. The second-order rate constant  $k_{\text{on}}^{15^\circ\text{C}} \approx 42$   $\text{M}^{-1} \text{s}^{-1}$  (molarity in per base) pertains over a 3-fold change in the concentration of  $d(\text{pA})_7$ , while maintaining the 2:1 ratio between  $d(\text{Tg})_4\text{-T-azido}$  and DNA. As expected, the first-order dissociation rate constant ( $k_{\text{off}}^{15^\circ\text{C}}$ ) does not change. The standard molar enthalpies,  $\Delta H^\circ(288) = E_{\text{on}} - E_{\text{off}}$ , are between  $-30$  and  $-60$  kcal/(mol base) and the standard free energies,  $\Delta G^\circ(288)$ , are between  $-8$  and  $-13$  kcal/(mol base) for short strands (5–10 base pairs) and have larger negative values at low ionic strength than at high ionic strength indicating that at lower  $\mu$  values the formation of triplexes of  $d(\text{Tg})_4\text{-T-azido}$  with  $d(\text{pA})_x$  is more favored. The  $\Delta H^\circ(288)$  and  $\Delta G^\circ(288)$  values also indicate a better stabilization of the  $(d(\text{Tg})_4\text{-T-azido})_2 \cdot d(\text{pA})_x$  complex as compared with triplexes of DNA.

**Acknowledgment.** This study was supported by the Office of Naval Research.

**Supporting Information Available:** Details of the determination of “on” and “off” rates (7 pages). See any current masthead for ordering and Internet access instructions.

(26) Sugimoto, N.; Nakano, S.-i.; Katoh, M.; Matsumura, A.; Nakamura, H.; Ohmichi, T.; Yoneyama, M.; Sasaki, M. *Biochemistry* **1995**, *34*, 11211.